Research Article

Gwanghyun Jo and Do Young Kwak*

A Reduced Crouzeix–Raviart Immersed Finite Element Method for Elasticity Problems with Interfaces

Abstract: The purpose of this paper is to develop a reduced Crouzeix–Raviart immersed finite element method (RCRIFEM) for two-dimensional elasticity problems with interface, which is based on the Kouhia–Stenberg finite element method (Kouhia et al. 1995) and Crouzeix–Raviart IFEM (CRIFEM) (Kwak et al. 2017). We use a P_1-conforming like element for one of the components of the displacement vector, and a P_1-nonconforming like element for the other component. The number of degrees of freedom of our scheme is reduced to two thirds of CRIFEM. Furthermore, we can choose penalty parameters independent of the Poisson ratio. One of the penalty parameters depends on Lamé's second constant μ, and the other penalty parameter is independent of both μ and λ. We prove the optimal order error estimates in piecewise H^1-norm, which is independent of the Poisson ratio. Numerical experiments show optimal order of convergence both in L^2 and piecewise H^1-norms for all problems including nearly incompressible cases.

Keywords: Immersed Finite Element Method, Elasticity Equation With Interface, Kouhia–Stenberg Element, Nearly Incompressible, Locking Free, Korn's Inequality

MSC 2010: 65N12, 65N30

1 Introduction

Linear elasticity equations, which describe the deformation of solid objects under the external force, play an important role in solid mechanics. One of the difficulties in solving the equations by finite element methods (FEMs) is that, when the material's Poisson ratio approaches $\frac{1}{2}$, the material becomes nearly incompressible. In this situation, the so-called "locking phenomenon" occurs for low-order standard nodal-based methods, i.e., they fail to converge to the correct solution. For example, for a linear element, FEM fails to converge to the solution when material is nearly incompressible. For the P_2 and P_3-conforming elements, the convergence orders tend to be suboptimal when the material is nearly incompressible [30]. On the other hand, a P_1-nonconforming element can not be used since it fails to satisfy Korn's inequality [11].

To overcome theses difficulties, several approaches were suggested. The nonconforming element of degree ≥ 2 converges uniformly [11] as the Poisson ratio approaches $\frac{1}{2}$. The mixed methods [7] can be applied to elasticity equations by introducing a new variable representing the divergence of the displacement. For a good review of mixed methods for linear elasticity, we refer to [29]. On the other hand, Kouhia and Stenberg (KS) introduced a new element which partially relaxes the continuity along the edges [16]. They use a P_1-conforming element for one component of the displacement and a P_1-nonconforming element

*Corresponding author: Do Young Kwak, Department of Mathematical Sciences, Korea Advanced Institute of Science and Technology, Daejeon, Republic of Korea, e-mail: kdy@kaist.ac.kr. http://orcid.org/0000-0002-5743-1501
Gwanghyun Jo, Department of Mathematics, Kunsan National University, Gunsan-si, Jeollabuk-do, Republic of Korea, e-mail: gwanghyun@kunsan.ac.kr. http://orcid.org/0000-0002-0635-2897

for the other. Recently, Hansbo introduced a nonconforming Galerkin method based on the Crouzeix–Raviart element with a stabilizing term [13].

Another difficulty that may arise in numerically solving the elasticity equations is that, when the material property changes across some interface, the Lamé constants become discontinuous. To solve such problems, FEMs are usually implemented with grids fitted to the interface.

On the other hand, there have been new developments for interface problems in the FEM community. We review two types of structured grids based methods. The first one is the extended finite element method (XFEM) [3, 4, 17, 22, 27] type, and the other one is the immersed finite element method (IFEM) [9, 14, 15, 18, 20, 21, 24, 25] type. In the XFEM type methods, one adds the enriched basis obtained by truncating the shape function along the interface. Therefore, extra degrees of freedom appear on each element cut by interface. In some cases, they remesh near the tip of crack.

IFEM, which allows the interface to cut through the elements, has been introduced by Z. Li, T. Lin and Y. Lin and their coworkers [24, 25], and its convergence behavior was investigated by Kwak et al. [9, 20] for elliptic problems. In IFEM type methods, we do not require extra degrees of freedom; instead, the basis functions are modified along the interface so that they satisfy the flux continuity conditions. One of the advantages of structured grid based methods is that we are free to use any regular grid for the interface problems. Thus, there is no need for grid generation. Furthermore, it is easy to develop fast solvers.

The Crouzeix–Raviart based IFEM (CRIFEM) for elasticity equations was recently developed in [14, 18, 21]. A rigorous error analysis was shown in [18], and the method was modified in [14] by adding the consistency terms. The advantage of the latter scheme is that we do not need extra regularity assumptions. For both methods, we observe the optimal order errors, even for the nearly incompressible case. For elasticity problems with spring-type non-homogeneous jumps [2], a scheme based on the concept of the discontinuous bubble [8] was developed in [21].

In this paper, we propose a new IFEM for linear elasticity equations having interfaces. First, we develop a new immersed finite element space based on KSFEM [16] and CRIFEM [18]. We use P_1-conforming like space for one of the displacement components, and P_1-nonconforming like space for the other. The KS basis functions are modified so that they satisfy the balance of traction along the interface. Next, we add a new penalty term which is different from the one in [13, 18, 28]. The advantage is that the parameters of the stabilizing terms are independent of λ which may approach infinity as the material becomes incompressible. We will call this method reduced Crouzeix–Raviart IFEM (RCRIFEM). We will prove the optimal order error estimates in piecewise H^1-norm, which is independent of the Poisson ratio. The total degrees of freedoms (dofs) of RCRIFEM are reduced to two thirds of the CRIFEM. Similar schemes can be derived for three-dimensional problems.

The rest of the paper is organized as follows. The governing equations of elasticity problems having an interface are described in Section 2. In Section 3, we develop a RCRIFEM for elasticity equations. In Section 4, we prove the optimal error estimates in piecewise H^1-norm independent of the Poisson ratio. The numerical results supporting our analysis are given in Section 5. The conclusion follows in Section 6.

2 Preliminaries

Let $\Omega = \Omega^+ \cup \Omega^-$ be a convex polygonal domain in $\mathbb{R}^2$ separated by a C^1-interface Γ (Figure 1). For convenience's sake, we assume Ω is a rectangular domain. We assume the subdomains Ω^+ and Ω^- are occupied by different elastic materials having distinct Lamé constants; $\mu = \mu^+$ and $\lambda = \lambda^+$ on Ω^+ and $\mu = \mu^-$ and $\lambda = \lambda^-$ on Ω^-.

We use the notation $\mathbf{u} = (u_1, u_2)$ for the displacement variable. We define the strain tensor $\boldsymbol{\epsilon}(\mathbf{u})$ and the stress tensor $\boldsymbol{\sigma}(\mathbf{u})$ as usual,

$$\boldsymbol{\epsilon}_{ij}(\mathbf{u}) = \frac{1}{2}\left(\frac{\partial u_i}{\partial x_j} + \frac{\partial u_j}{\partial x_i}\right), \quad \boldsymbol{\sigma}(\mathbf{u}) = 2\mu\boldsymbol{\epsilon}(\mathbf{u}) + \lambda\,\mathrm{tr}(\boldsymbol{\epsilon}(\mathbf{u}))\mathbf{I},$$

where $\mathbf{I}$ is a 2×2 identity matrix.
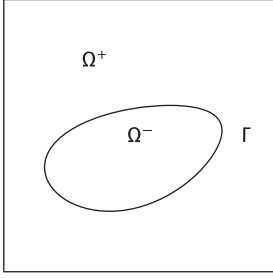
Figure 1: A domain Ω with interface.

The governing equation of the elasticity with an interface on the heterogeneous domain Ω is

$$-\operatorname{div}\boldsymbol{\sigma}(\mathbf{u}) = \mathbf{f} \quad \text{in } \Omega^{\pm}, \tag{2.1a}$$

$$[\mathbf{u}]_{\Gamma} = 0, \tag{2.1b}$$

$$[\boldsymbol{\sigma}(\mathbf{u})\cdot\mathbf{n}]_{\Gamma} = 0, \tag{2.1c}$$

$$\mathbf{u} = 0 \quad \text{in } \partial\Omega, \tag{2.1d}$$

where $\mathbf{f} \in [L^2(\Omega)]^2$ is an external force and the bracket $[\cdot]_{\Gamma}$ means the jump across the interface, i.e., $[\mathbf{u}]_{\Gamma} := \mathbf{v}|_{\Omega^+} - \mathbf{v}|_{\Omega^-}$. Equation (2.1c) is the balance of traction. The Lamé constants μ and λ are given in terms of modulus of elasticity $E > 0$ and Poisson's ratio $0 < \nu < \frac{1}{2}$,

$$\mu = \frac{E}{2(1+\nu)}, \quad \lambda = \frac{E\nu}{(1+\nu)(1-2\nu)}.$$

We note that, as $\nu \to \frac{1}{2}$, the parameter λ goes to infinity in the incompressible case. We assume that μ is bounded by two positive constants $\underline{\mu}$ and $\overline{\mu}$ such that $0 < \underline{\mu} \le \mu \le \overline{\mu}$.

We introduce Sobolev spaces and their norms. Let $p \ge 1$ and $m \ge 0$ be integers. For any domain D, we let $W_p^m(D)$ be the usual Sobolev space with (semi-)norms denoted by $|\cdot|_{m,p,D}$ and $\|\cdot\|_{m,p,D}$. Let $H^m(D) = W_2^m(D)$ with (semi-)norms denoted by $|\cdot|_{m,D} = |\cdot|_{m,2,D}$ and $\|\cdot\|_{m,D} = \|\cdot\|_{m,2,D}$. Let

$$(H_0^1(\Omega))^2 = \{\mathbf{u} \in (H^1(\Omega))^2 : \mathbf{u} = 0 \text{ on } \partial\Omega\}.$$

The following regularity result is well known from [12, 23].

Theorem 2.1. *There exists a unique* $\mathbf{u} \in (H_0^1(\Omega))^2 \cap (H^2(\Omega^+))^2 \cap (H^2(\Omega^-))^2$, *satisfying* (2.1).

Remark 2.2. In fact, the convexity assumption on the domain is only necessary to ensure $\mathbf{u} \in (H^2(\Omega^s))^2$, $s = \pm$. When the domain is nonconvex polygon, one can only guarantee that $\mathbf{u} \in (H^{1+\epsilon}(\Omega^s))^2$, $s = \pm$, for some $0 < \epsilon < 1$. In this case, even the standard FEM using fitted grid produces $O(h^\epsilon)$ error in H^1-norm. Our scheme to be presented below should have the same effect for nonconvex domain.

3 RCRIFEM for Elasticity Equation with Interface

3.1 RCRIFEM Space

Let $\mathcal{T}_h$ be a triangulation of Ω by triangles not necessarily aligning with the interface. We define local spaces on each element $T \in \mathcal{T}_h$. Let $S_h(T)$ be the space of P_1 functions defined by vertex dof, and let $N_h(T)$ be the space of P_1 functions defined by edge average dof. We first recall the KS space for elasticity problems having continuous material constants in [16]. For any function $\phi \in H^1(T)$, let $\overline{\phi}$ be the edge average function along an edge e of T defined by

$$\overline{\phi}|_e = \frac{1}{|e|}\int_e \phi \, ds.$$
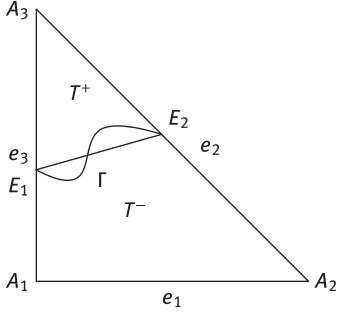
Figure 2: A typical interface triangle.

Here, $|e|$ is the Lebesgue measure of e. With the local space given by $\mathbf{U}_h(T) := N_h(T) \times S_h(T)$, the global space is defined by

$$
\mathbf{U}_h = \left\{
\begin{array}{l}
\boldsymbol{\phi}_h = (\phi_{h,1}, \phi_{h,2}) \in \mathbf{U}_h(T) \text{ for any } T \in \mathcal{T}_h, \\[4pt]
\displaystyle\int_e \phi_{h,1}|_{T_1} = \int_e \phi_{h,1}|_{T_2}, \text{ where } e \text{ is a common edge of } T_1 \text{ and } T_2, \\[4pt]
\phi_{h,2} \text{ is continuous on each vertex of } T \in \mathcal{T}_h, \\[4pt]
\overline{\phi_{h,1}}|_{\partial T \cap \partial \Omega} = \phi_{h,2} = 0 \text{ for any } T \in \mathcal{T}_h
\end{array}
\right\}.
$$

Now, we define a RCRIFEM space by modifying the basis function of KS element. We call T an interface element if the interface intersects the interior of T; otherwise, T is called a noninterface element. We assume that the interface intersects an element at no more than two points, which are satisfied when h is small enough. Suppose T is an interface element with vertices A_i, $i = 1, 2, 3$, having E_1 and E_2 as points of intersections of Γ and edges (Figure 2). We let T^+ and T^- be the two regions separated by $\overline{E_1 E_2}$. For a given function $\boldsymbol{\phi} = (\phi_1, \phi_2) \in \mathbf{U}_h(T)$, we modify it so that the new function $\widehat{\boldsymbol{\phi}}$ is a piecewise linear vector function on T given by

$$
\widehat{\boldsymbol{\phi}} =
\begin{cases}
\begin{pmatrix} \widehat{\phi}_1^+ \\ \widehat{\phi}_2^+ \end{pmatrix} = \begin{pmatrix} a_1^+ + b_1^+ x + c_1^+ y \\ a_2^+ + b_1^+ x + c_2^+ y \end{pmatrix}, & (x, y) \in T^+, \\[12pt]
\begin{pmatrix} \widehat{\phi}_1^- \\ \widehat{\phi}_2^- \end{pmatrix} = \begin{pmatrix} a_1^- + b_1^- x + c_1^- y \\ a_2^- + b_2^- x + c_2^- y \end{pmatrix}, & (x, y) \in T^-.
\end{cases}
\tag{3.1}
$$

The coefficients in (3.1) are determined by the edge averages for $\widehat{\phi}_1$, the nodal values for $\widehat{\phi}_2$, and the interface conditions (2.1b), (2.1c) as follows:

$$
\overline{\widehat{\phi}_1}|_{e_i} = \overline{\phi_1}|_{e_i}, \qquad i = 1, 2, 3, \tag{3.2a}
$$

$$
\widehat{\phi}_2(A_i) = \phi_2(A_i), \qquad i = 1, 2, 3, \tag{3.2b}
$$

$$
\widehat{\boldsymbol{\phi}}^-(E_i) = \widehat{\boldsymbol{\phi}}^+(E_i), \qquad i = 1, 2, \tag{3.2c}
$$

$$
\int_{\overline{E_1 E_2}} \boldsymbol{\sigma}(\widehat{\boldsymbol{\phi}})^- \cdot \mathbf{n}_{\overline{E_1 E_2}} = \int_{\overline{E_1 E_2}} \boldsymbol{\sigma}(\widehat{\boldsymbol{\phi}})^+ \cdot \mathbf{n}_{\overline{E_1 E_2}}, \tag{3.2d}
$$

where

$$
\boldsymbol{\sigma}(\widehat{\boldsymbol{\phi}})^- = 2\mu^- \boldsymbol{\epsilon}(\widehat{\boldsymbol{\phi}}) + \lambda^- \operatorname{div} \widehat{\boldsymbol{\phi}},
$$

$$
\boldsymbol{\sigma}(\widehat{\boldsymbol{\phi}})^+ = 2\mu^+ \boldsymbol{\epsilon}(\widehat{\boldsymbol{\phi}}) + \lambda^+ \operatorname{div} \widehat{\boldsymbol{\phi}}.
$$

Proposition 3.1. *The function $\widehat{\boldsymbol{\phi}}$ in (3.1) is determined uniquely by conditions (3.2).*

Proof. See the appendix. □

When T is an interface element, we define the local immersed finite element space $\widehat{\mathbf{U}}_h(T)$ as a set of piecewise linear functions $\widehat{\boldsymbol{\phi}}$ in the form of (3.1) satisfying conditions (3.2). The global immersed finite element

space $\widehat{\mathbf{U}}_h$ is defined as the set of functions $\boldsymbol{\phi} = (\phi_1, \phi_2)$ in $L^2(\Omega)$ satisfying the following conditions:

$$
\begin{cases}
\boldsymbol{\phi}|_T \in \mathbf{U}_h(T) & \text{if } T \text{ is a noninterface element,} \\
\boldsymbol{\phi}|_T \in \widehat{\mathbf{U}}_h(T) & \text{if } T \text{ is an interface element,} \\
\int_e \phi_{h,1}|_{T_1} = \int_e \phi_{h,1}|_{T_2} & \text{if } e \text{ is the common edges of } T_1 \text{ and } T_2, \\
\phi_{h,2}|_{T_1} = \phi_{h,2}|_{T_2} & \text{at common nodes of } T_1 \text{ and } T_2, \\
\overline{\phi_{h,1}}|_e = 0 & \text{if } e \in \partial T \text{ is a part of the boundary } \partial\Omega, \\
\phi_{h,2} = 0 & \text{at the boundary edges.}
\end{cases}
$$

Next, we show in the following lemma that the modified basis function $\widehat{\boldsymbol{\phi}} \in \widehat{\mathbf{U}}_h$ weakly satisfies the balance of traction condition (2.1c) on the curve $T \cap \Gamma$ for every interface element $T \in \mathcal{T}_h$.

Lemma 3.2. *For an interface element T, the following conditions are equivalent for a continuous piecewise linear function $\boldsymbol{\phi}$:*

$$
\int_{\Gamma \cap T} (\boldsymbol{\sigma}(\boldsymbol{\phi})^+ - \boldsymbol{\sigma}(\boldsymbol{\phi})^-) \cdot \mathbf{n}_\Gamma \, ds = 0,
$$

$$
\int_{\overline{E_1 E_2}} (\boldsymbol{\sigma}(\boldsymbol{\phi})^+ - \boldsymbol{\sigma}(\boldsymbol{\phi})^-) \cdot \mathbf{n}_{\overline{E_1 E_2}} \, ds = 0.
$$

Proof. This can be proved by Green's theorem and the fact that divergence of a $\boldsymbol{\sigma}(\boldsymbol{\phi})$ is zero. □

3.2 The Associated Variational Form

We define the associated variational form for problem (2.1). By multiplying $v \in \mathbf{H}_h(\Omega) := \widehat{\mathbf{U}}_h + (H_0^1(\Omega))^2$ to (2.1a) and integrating by parts on each element $T \in \mathcal{T}_h$, we see that the weak problem becomes

$$
a(\mathbf{u}, \mathbf{v}) = (f, \mathbf{v}),
$$

where

$$
a(\mathbf{u}, \mathbf{v}) = \sum_{T \in \mathcal{T}_h} \int_T 2\mu\boldsymbol{\epsilon}(\mathbf{u}) : \boldsymbol{\epsilon}(\mathbf{v}) + \sum_T \int_T \lambda \operatorname{div} \mathbf{u} \operatorname{div} \mathbf{v} - \sum_{e \in \mathcal{E}_h} \int_e \{\boldsymbol{\sigma}(\mathbf{u}) \cdot \mathbf{n}\}[\mathbf{v}]
$$

and $(\cdot, \cdot)$ is the L^2 inner product on Ω. Here, $\mathcal{E}_h$ is the set of interior edges of $\mathcal{T}_h$. In order to develop an FEM discretization, we need to add stability terms $\sum_{e \in \mathcal{E}_h} \frac{\tau_1}{|e|} \int_e [\mathbf{u}][\mathbf{v}]$ and $\sum_{e \in \mathcal{E}_h} \frac{\tau_2}{|e|} \int_e [\mathbf{u} \cdot \mathbf{n}][\mathbf{v} \cdot \mathbf{n}]$. Without the stability terms, the form $a(\cdot, \cdot)$ will not be coercive. Also, an optional symmetric term $\epsilon \sum_{e \in \mathcal{E}_h} \int_e \{\boldsymbol{\sigma}(\mathbf{v}) \cdot \mathbf{n}\}[\mathbf{u}]$ is added to ensure symmetry as in the usual discontinuous Galerkin (DG) formulations. Thus, we define a bilinear form $a_h(\cdot, \cdot)$ on $\mathbf{H}_h(\Omega) \times \mathbf{H}_h(\Omega)$ by

$$
a_h(\mathbf{u}, \mathbf{v}) := \sum_{T \in \mathcal{T}_h} \int_T 2\mu\boldsymbol{\epsilon}(\mathbf{u}) : \boldsymbol{\epsilon}(\mathbf{v}) + \sum_T \int_T \lambda \operatorname{div} \mathbf{u} \operatorname{div} \mathbf{v} - \sum_{e \in \mathcal{E}_h} \int_e \{\boldsymbol{\sigma}(\mathbf{u}) \cdot \mathbf{n}\}[\mathbf{v}]
$$
$$
+ \epsilon \sum_{e \in \mathcal{E}_h} \int_e \{\boldsymbol{\sigma}(\mathbf{v}) \cdot \mathbf{n}\}[\mathbf{u}] + \sum_{e \in \mathcal{E}_h} \frac{\tau_1}{|e|} \int_e [\mathbf{u}][\mathbf{v}] + \sum_{e \in \mathcal{E}_h} \frac{\tau_2}{|e|} \int_e [\mathbf{u} \cdot \mathbf{n}][\mathbf{v} \cdot \mathbf{n}]. \tag{3.3}
$$

The bilinear form is similar to the DG case, corresponding to NIPG, IIPG and SIPG when $\epsilon = 1$, $\epsilon = 0$, $\epsilon = -1$ respectively. However, the degrees of freedom are not completely free, i.e., dofs of the first component are continuous across edges of elements and those of the second component have common vertex values. We note that the functions in IFEM spaces are discontinuous along the interface edges. Because of the discontinuity of the basis in $\widehat{\mathbf{U}}_h$, scheme (3.3) is inconsistent without the third and fourth terms of the right-hand side. As we will show, the terms related to consistency errors in (3.3) play important roles in the error analysis. In fact, these kinds of terms were introduced for the IFEM in [19, 26] and were shown to enhance the accuracy of the IFEM for the scalar elliptic interface problems. We note that, when μ is continuous, these terms vanish naturally as in the standard FEM schemes, and the scheme reduces to the similar KSFEM in [16].

If $\tau_2 = 0$, $a_h(\cdot, \cdot)$ has the same form as the CRIFEM introduced in [14], where a Crouzeix–Raviart type of IFEM space is used for both components. In [14], the choice of τ_1 was ad hoc. In this work, we are able to show that the threshold values of τ_1 and τ_2 to ensure coerciveness are bounded as λ goes to infinity. In fact, τ_1 is dependent only on μ, and τ_2 is independent of both μ and λ.

Our RCRIFEM is based on the bilinear form (3.3): find $\mathbf{u}_h \in \widehat{\mathbf{U}}_h$ such that

$$a_h(\mathbf{u}_h, \mathbf{v}_h) = (\mathbf{f}, \mathbf{v}_h) \quad \text{for all } \mathbf{v}_h \in \widehat{\mathbf{U}}_h. \tag{3.4}$$

The following result is immediate.

Proposition 3.3. *The RCRIFEM scheme is consistent in the sense that if* $\mathbf{u}$ *is the solution of* (2.1), *then*

$$a_h(\mathbf{u}, \mathbf{v}_h) = (\mathbf{f}, \mathbf{v}_h)$$

holds for all $\mathbf{v}_h \in \mathbf{H}_h(\Omega)$.

4 Error Analysis

First, we introduce broken function spaces and norms. For $m = 1, 2$ and any domain $D = T \in \mathcal{T}_h$ or $D = \Omega$, let

$$(\widetilde{H}^m(D))^2 := \{\mathbf{u} \in (H^{m-1}(D))^2 : \mathbf{u}|_{D \cap \Omega^s} \in (H^m(D \cap \Omega^s))^2, \ s = +, -\},$$

with norms

$$|\mathbf{u}|^2_{\widetilde{H}^m(D)} := |\mathbf{u}|^2_{m, D \cap \Omega^+} + |\mathbf{u}|^2_{m, D \cap \Omega^-} \quad \text{and} \quad \|\mathbf{u}\|^2_{\widetilde{H}^m(D)} := \|\mathbf{u}\|^2_{m-1, D} + |\mathbf{u}|^2_{\widetilde{H}^m(D)}.$$

We define piecewise Sobolev (semi-)norms $\|\cdot\|_{m, h}$ and energy-like norms $\|\cdot\|_{E_h(\Omega)}$ for $\mathbf{u} \in \mathbf{H}_h(\Omega)$,

$$\|\mathbf{u}\|^2_{m, h} = \sum_{T \in \mathcal{T}_h} \|\mathbf{u}\|^2_{\widetilde{H}^m(T)}, \quad |\mathbf{u}|^2_{m, h} = \sum_{T \in \mathcal{T}_h} |\mathbf{u}|^2_{\widetilde{H}^m(T)}, \quad \text{and} \quad \|\mathbf{u}\|^2_{E_h} := \sum_{T \in \mathcal{T}_h} \|\mathbf{u}\|^2_{E, T},$$

where

$$\|\mathbf{u}\|^2_{E, T} := \|\boldsymbol{\epsilon}(\mathbf{u})\|^2_{0, T} + \|\sqrt{\lambda} \operatorname{div} \mathbf{u}\|^2_{0, T} + h^{-1} \sum_{e \in \partial T \cap \mathcal{E}_h} (\|[\mathbf{u}]\|^2_{0, e} + \|[\mathbf{u} \cdot \mathbf{n}_e]\|^2_{0, e}).$$

We need subspaces of $(\widetilde{H}^2(T))^2$ and $(\widetilde{H}^2(\Omega))^2$ satisfying the jump conditions

$$(\widetilde{H}^2_\Gamma(T))^2 := \{\mathbf{u} \in (\widetilde{H}^2(T))^2 : [\boldsymbol{\sigma}(\mathbf{u}) \cdot \mathbf{n}]_{\Gamma \cap T} = 0\},$$

$$(\widetilde{H}^2_\Gamma(\Omega))^2 := \{\mathbf{u} \in (\widetilde{H}^1_0(\Omega))^2 : \mathbf{u} \in (\widetilde{H}^2_\Gamma(T))^2 \text{ for all } T \in \mathcal{T}_h\}.$$

Throughout the paper, the generic constants C are independent of h and λ.

4.1 Approximation Property of $\widehat{\mathbf{U}}_h$

In this subsection, we study the approximation property of $\widehat{\mathbf{U}}_h$ by proving the interpolation error. One of the difficulties in proving the interpolation error is that the space $\widehat{\mathbf{U}}_h(T)$ is not a subspace of $(\widetilde{H}^2_\Gamma(T))^2$ when the interface is not piecewise linear. To overcome this difficulty, we introduce a bigger space which contains both $\widehat{\mathbf{U}}_h(T)$ and $(\widetilde{H}^2_\Gamma(T))^2$. First we note that replacing the interface by a piecewise linear approximation will affect the interpolation error only by an order of $O(h^2)$ (see, for example, [5]).

Suppose T is an interface element with curved interface Γ. Let (see Figure 3)

$$T_r = T - \Omega^- \cap T^+ - \Omega^+ \cap T^- \quad \text{and} \quad T_r^s = T_r \cap \Omega^s, \quad s = -, +.$$

We define

$$X(T) := \{\mathbf{u} : \mathbf{u} \in (H^1(T))^2, \ \mathbf{u} \in (H^2(S))^2 \text{ for all } S = T_r^+, T_r^-, T^+ \cap \Omega^+, T^- \cap \Omega^-\},$$

$$X_\Gamma(T) := \left\{\mathbf{u} \in X(T), \ \int_{\Gamma \cap T} (\boldsymbol{\sigma}(\mathbf{u})^+ - \boldsymbol{\sigma}(\mathbf{u})^-) \cdot \mathbf{n}_\Gamma \, ds = 0\right\},$$

where $\boldsymbol{\sigma}(\mathbf{u})^- = 2\mu^- \boldsymbol{\epsilon}(\mathbf{u}) + \lambda^- \operatorname{div} \mathbf{u}$, $\boldsymbol{\sigma}(\mathbf{u})^+ = 2\mu^+ \boldsymbol{\epsilon}(\mathbf{u}) + \lambda^+ \operatorname{div} \mathbf{u}$.
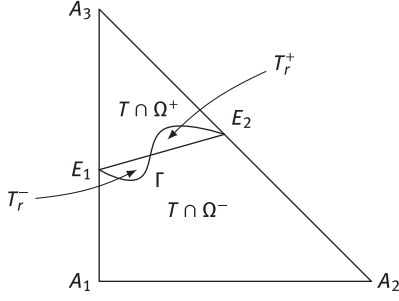
Figure 3: Typical interface element.

Note the relations

$$(\widetilde{H}^2(T))^2 \hookrightarrow X(T) \hookrightarrow (H^1(T))^2,$$

$$(\widetilde{H}_\Gamma^2(T))^2 \cup \widehat{\mathbf{U}}_h(T) \hookrightarrow X_\Gamma(T) \hookrightarrow X(T) \hookrightarrow (H^1(T))^2.$$

For any $\mathbf{u} \in X(T)$, we define the norms

$$|\mathbf{u}|_{X(T)}^2 = |\mathbf{u}|_{2,T^-\cap\Omega^-}^2 + |\mathbf{u}|_{2,T^+\cap\Omega^+}^2 + |\mathbf{u}|_{2,T_r^-}^2 + |\mathbf{u}|_{2,T_r^+}^2,$$

$$\|\mathbf{u}\|_{X(T)}^2 = \|\mathbf{u}\|_{1,T}^2 + |\mathbf{u}|_{X(T)}^2 + \|\sqrt{\lambda}\,\mathrm{div}\,\mathbf{u}\|_{0,T}^2 + |\sqrt{\lambda}\,\mathrm{div}\,\mathbf{u}|_{1,T^+}^2 + |\sqrt{\lambda}\,\mathrm{div}\,\mathbf{u}|_{1,T^-}^2,$$

$$\|\mathbf{u}\|_{2,T}^2 = |\mathbf{u}|_{X(T)}^2 + |\sqrt{\lambda}\,\mathrm{div}\,\mathbf{u}|_{1,T^+}^2 + |\sqrt{\lambda}\,\mathrm{div}\,\mathbf{u}|_{1,T^-}^2$$
$$+ \left| \int_{\Gamma\cap T} (\boldsymbol{\sigma}(\boldsymbol{\phi})^+ - \boldsymbol{\sigma}(\boldsymbol{\phi})^-) \cdot \mathbf{n}_\Gamma \, ds \right|^2 + \sum_{i=1}^{3} |\overline{u_1}|_{e_i}|^2 + \sum_{i=1}^{3} |u_2(A_i)|^2.$$

We now prove the approximation property.

Lemma 4.1. $\|\!|\cdot|\!\|_{2,T}$ *is a norm on the space $X_\Gamma(T)$ which is equivalent to $\|\cdot\|_{X(T)}$.*

Proof. Assume $\mathbf{u} \in X_\Gamma(T)$ satisfies $\|\!|\cdot|\!\|_{2,T} = 0$. Since $|\mathbf{u}|_{X(T)} = 0$, $\mathbf{u}$ is linear on each of the four regions $T^- \cap \Omega^-$, $T^+ \cap \Omega^+$, T_r^- and T_r^+. Since $\mathbf{u} \in H^1(T)$, $\mathbf{u}$ is continuous on T. By Lemma 3.2 and the fact that $\int_{T\cap\Gamma} [\boldsymbol{\sigma}(\mathbf{u}) \cdot \mathbf{n}_\Gamma] \, ds = 0$, $\mathbf{u}$ satisfies the interface condition along the line segment $\overline{E_1 E_2}$. This implies $\mathbf{u} \in \widehat{\mathbf{U}}_h(T)$ and together with the conditions $\overline{u_1}|_{e_i} = 0$, $i = 1, 2, 3$, and $u_2(A_i) = 0$, $i = 1, 2, 3$, we conclude that $\mathbf{u} = 0$, which shows that $\|\!|\cdot|\!\|_{2,T}$ is a norm.

Next, we show the equivalence of $\|\cdot\|_{X(T)}$ and $\|\!|\cdot|\!\|_{2,T}$. By the Sobolev embedding theorem that $H^2(S)$ is compactly embedded in $C^0(S)$ for subregion S of T, we see that

$$\sum_{i=1}^{3} |\overline{u_1}|_{e_i}| + \sum_{i=1}^{3} |u_2(A_i)| \le C \max_{S\in B} \|\mathbf{u}\|_{L^\infty(S)} \le C \max_{S\in B} \|\mathbf{u}\|_{H^2(S)} \le C\|\mathbf{u}\|_{\widetilde{H}^2(T)} \le C\|\mathbf{u}\|_{X(T)},$$

where $B = \{T_r^+, T_r^-, T^+ \cap \Omega^+, T^- \cap \Omega^-\}$. Hence, we see that

$$\|\!|\mathbf{u}|\!\|_{2,T} \le C\|\mathbf{u}\|_{X(T)}.$$

The converse can be proved similarly to [18]. $\square$

We define an interpolation operator: for any $\mathbf{u} \in (\widetilde{H}^2(T))^2$, we define $I_h\mathbf{u} \in \widehat{\mathbf{U}}_h(T)$ using the average values of u_1 and node values of u_2 on each edge of T by

$$\int_{e_i} (I_h u)_1 \, ds = \int_{e_i} u_1 \, ds, \quad i = 1, 2, 3,$$

$$(I_h u)_2(A_i) = u_2(A_i), \quad i = 1, 2, 3,$$

and call $I_h\mathbf{u}$ the interpolant of $\mathbf{u}$ in $\widehat{\mathbf{U}}_h(T)$. We extend the definition of I_h for $\mathbf{u} \in (\widetilde{H}^2(\Omega))^2$ by $(I_h\mathbf{u})_T = I_h(\mathbf{u}|_T)$ for each $T \in \mathcal{T}_h$.

Lemma 4.2. *For any* $\mathbf{u} \in (\widetilde{H}_\Gamma^2(T))^2$, *there exists a constant* $C > 0$ *such that, for* $m = 0, 1$,

$$\|\mathbf{u} - I_h\mathbf{u}\|_{m,T} + m \cdot \|\sqrt{\lambda}(\mathbf{u} - I_h\mathbf{u})\|_{L^2(T)} \leq Ch^{2-m}(\|\mathbf{u}\|_{\widetilde{H}^2(T)} + m \cdot \|\sqrt{\lambda}\operatorname{div}\mathbf{u}\|_{\widetilde{H}^1(T)}),$$

$$\|\mathbf{u} - I_h\mathbf{u}\|_{m,T} \leq Ch^{2-m}\|\mathbf{u}\|_{\widetilde{H}^2(T)}.$$

Proof. The proof follows by the definition of interpolant, $\|\cdot\|_{X(T)}$, $\||\cdot\||_{2,h}$, Lemma 4.1 and a scaling argument [18]. □

A similar estimate holds with the energy-like norm.

Theorem 4.3. *For any* $\mathbf{u} \in (\widetilde{H}_\Gamma^2(\Omega))^2$, *there exists a constant* $C_I > 0$ *such that*

$$\|\mathbf{u} - I_h\mathbf{u}\|_{E_h} \leq C_I h(\|\mathbf{u}\|_{\widetilde{H}^2(\Omega)} + \|\sqrt{\lambda}\operatorname{div}\mathbf{u}\|_{\widetilde{H}^1(\Omega)})$$

Proof. Given T in $\mathcal{T}_h$, we denote the union of all neighboring elements of $T \in \mathcal{T}_h$ including T by T^O. Let T_e be the neighboring element of T having e as a common edge. For the last two terms of $\|\mathbf{u} - \mathbf{u}_h\|_{E,T}$, we have

$$\frac{1}{h}\big(\|[\mathbf{u} - I_h\mathbf{u}]\|_{0,e}^2 + \|[(\mathbf{u} - I_h\mathbf{u}) \cdot \mathbf{n}_e]\|_{0,e}^2\big)$$

$$\leq C\Big(\frac{1}{h}\|(\mathbf{u} - I_h\mathbf{u})|_T\|_{0,e}^2 + \frac{1}{h}\|(\mathbf{u} - I_h\mathbf{u})|_{T_e}\|_{0,e}^2\Big)$$

$$\leq C\Big(\frac{1}{h^2}\|\mathbf{u} - I_h\mathbf{u}\|_{0,T}^2 + |\mathbf{u} - I_h\mathbf{u}|_{1,T}^2 + \frac{1}{h^2}\|\mathbf{u} - I_h\mathbf{u}\|_{0,T_e}^2 + |\mathbf{u} - I_h\mathbf{u}|_{1,T_e}^2\Big)$$

$$\leq Ch^2\|\mathbf{u}\|_{\widetilde{H}^2(T^O)}^2$$

by the trace inequality and Lemma 4.2. Hence, by the definition of $\|\cdot\|_{E,T}$ and by Lemma 4.2, we have

$$\|\mathbf{u} - I_h\mathbf{u}\|_{E,T} \leq C(\|\mathbf{u} - I_h\mathbf{u}\|_{1,T} + \|\sqrt{\lambda}\operatorname{div}(\mathbf{u} - I_h\mathbf{u})\|_{L^2(T)} + h\|\mathbf{u}\|_{\widetilde{H}^2(T^O)})$$

$$\leq Ch(\|\mathbf{u}\|_{\widetilde{H}^2(T)} + \|\sqrt{\lambda}\operatorname{div}\mathbf{u}\|_{\widetilde{H}^1(T)} + \|\mathbf{u}\|_{\widetilde{H}^2(T^O)}).$$

Summing over T completes the proof. □

Remark 4.4. The above lemma was proved for the case of a line segment.

4.2 H^1-Error Estimate

We first show that the piecewise H^1-norm is bounded by $\|\cdot\|_{E_h}$, and we proceed the analysis using the $\|\cdot\|_{E_h}$ norm. We need the discrete Poincaré inequality.

Lemma 4.5. *There exists a constant* $C > 0$ *such that, for any* $\mathbf{v}_h \in \widehat{\mathbf{U}}_h$,

$$C\|\mathbf{v}_h\|_{L^2(\Omega)}^2 \leq |\mathbf{v}_h|_{1,h}^2. \tag{4.1}$$

Proof. This can be proved with similar techniques as in [9, 20]. □

We need the discrete Korn inequality for piecewise H^1-vector fields to bound the broken H^1-semi-norm by the energy-like norm $\|\cdot\|_{E_h}$.

Lemma 4.6 ([6, 10]). *There exists a constant* $C > 0$ *such that*

$$|\mathbf{v}_h|_{1,h}^2 \leq C\Big(\sum_{T \in \mathcal{T}_h}(\|\boldsymbol{\epsilon}(\mathbf{v}_h)\|_{0,T}^2 + \|Q(\mathbf{v}_h)\|_{0,T}^2) + \sum_{e \in \mathcal{E}_h}\frac{\tau_1}{|e|}\int_e[\mathbf{v}_h]^2\,\mathrm{d}s\Big)$$

for all $\mathbf{v}_h \in \widehat{\mathbf{U}}_h$, *where* $Q(\mathbf{v}_h) := \mathbf{v}_h - \frac{1}{|T|}\int_T \mathbf{v}_h\,\mathrm{d}x$.

Corollary 4.7. *There exists* $C > 0$ *such that* $\|\mathbf{v}_h\|_{1,h}^2 \leq C\|\mathbf{v}_h\|_{E_h}^2$ *holds for all* $\mathbf{v}_h \in \widehat{\mathbf{U}}(T)$ *when* $h > 0$ *is sufficiently small.*

Proof. Given $T \in \mathfrak{T}_h$, since $\widehat{\mathbf{U}}_h(T) \in (H^1(T))^2$, there exists $C > 0$ such that $\|Q(\mathbf{v}_h)\|_{0,T}^2 \leq Ch^2|\mathbf{v}_h|_{1,T}^2$ holds. Hence, by Lemma 4.6, we have $|\mathbf{v}_h|_{1,h}^2 \leq C\|\mathbf{v}_h\|_{E_h}^2$ for all sufficiently small $h > 0$. Hence, by the discrete Poincaré inequality (4.1), we obtain the result. $\qquad\square$

Now, we show the coerciveness of $a_h(\cdot, \cdot)$ as defined in (3.3). Let C_N be the number of maximum neighbors that one element can meet in the triangulation $\mathfrak{T}_h$.

Lemma 4.8. *If τ_1 and τ_2 are sufficiently large, then there exists a constant C_A such that $C_A\|\mathbf{v}_h\|_{E_h}^2 \leq a_h(\mathbf{v}_h, \mathbf{v}_h)$ holds for all $\mathbf{v}_h \in \widehat{\mathbf{U}}_h$.*

Proof. When $\epsilon = 1$, there is nothing to prove. Suppose $\epsilon = -1$ or $\epsilon = 0$. It suffices to bound the third and fourth terms of $a_h(\mathbf{v}_h, \mathbf{v}_h)$ in (3.3). The third term of $a_h(\mathbf{v}_h, \mathbf{v}_h)$ is written as

$$\sum_{e \in \mathcal{E}_h} \int_e \{\boldsymbol{\sigma}(\mathbf{v}_h) \cdot \mathbf{n}\}[\mathbf{v}_h]\,ds = \sum_{e \in \mathcal{E}_h} \int_e \mu\{\boldsymbol{\epsilon}(\mathbf{v}_h) \cdot \mathbf{n}\}[\mathbf{v}_h]\,ds + \sum_{e \in \mathcal{E}_h} \int_e \lambda\{\mathrm{div}(\mathbf{v}_h) \cdot \mathbf{n}\}[\mathbf{v}_h]\,ds. \tag{4.2}$$

By the Cauchy–Schwarz inequality, the first term of (4.2) is bounded as

$$\sum_{e \in \mathcal{E}_h} \int_e |\mu\{\boldsymbol{\epsilon}(\mathbf{v}_h) \cdot \mathbf{n}\}[\mathbf{v}_h]\,ds| \leq \sum_{e \in \mathcal{E}_h} (h\overline{\mu}\|\{\boldsymbol{\epsilon}(\mathbf{v}_h) \cdot \mathbf{n}\}\|_{0,e}^2)^{\frac{1}{2}} (h^{-1}\|[\mathbf{v}_h]\|_{0,e}^2)^{\frac{1}{2}}.$$

However, using the similar techniques in [19], we can prove that there exists $C_0 > 0$ such that, for all $\mathbf{v}_h \in \widehat{U}_h$ and for all $T \in \mathfrak{T}$,

$$h\|\{\boldsymbol{\epsilon}(\mathbf{v}_h) \cdot \mathbf{n}\}\|_{0,e}^2 \leq C_0\|\boldsymbol{\epsilon}(\mathbf{v}_h)\|_{0,T}^2$$

holds, where $e \in \partial T$ is an edge of T. Thus, by Young's inequality, we have

$$\sum_{e \in \mathcal{E}_h} \int_e |\mu\{\boldsymbol{\epsilon}(\mathbf{v}_h) \cdot \mathbf{n}\}[\mathbf{v}_h]\,ds| \leq \Big(\sum_{T \in \mathfrak{T}_h} \overline{\mu}C_N C_0\|\boldsymbol{\epsilon}(\mathbf{v}_h)\|_{0,T}^2\Big)^{\frac{1}{2}} \Big(\sum_{e \in \mathcal{E}_h} h^{-1}\|[\mathbf{v}_h]\|_{0,e}^2\Big)^{\frac{1}{2}}$$

$$\leq \frac{\gamma_1}{2}\Big(\sum_{T \in \mathfrak{T}_h} \|\boldsymbol{\epsilon}(\mathbf{v}_h)\|_{0,T}^2\Big) + \frac{\overline{\mu}C_N C_0}{2\gamma_1}\Big(\sum_{e \in \mathcal{E}_h} h^{-1}\|[\mathbf{v}_h]\|_{0,e}^2\Big) \quad \text{for any } \gamma_1 > 0.$$

Similarly,

$$\sum_{e \in \mathcal{E}_h} \int_e |\lambda\{\mathrm{div}(\mathbf{v}_h)I \cdot \mathbf{n}\}[\mathbf{v}_h]\,ds| = \sum_{e \in \mathcal{E}_h} \int_e |\lambda\{\mathrm{div}(\mathbf{v}_h)\}[\mathbf{v}_h \cdot \mathbf{n}]\,ds|$$

$$\leq \frac{\gamma_2}{2}\Big(\sum_{T \in \mathfrak{T}_h} \|\sqrt{\lambda}\,\mathrm{div}\,\mathbf{v}_h\|_{0,T}^2\Big) + \frac{C_N C_0}{2\gamma_2}\Big(\sum_{e \in \mathcal{E}_h} h^{-1}\|[\mathbf{v}_h \cdot \mathbf{n}]\|_{0,e}^2\Big) \quad \text{for any } \gamma_2 > 0.$$

Hence, we have

$$a_h(\mathbf{v}, \mathbf{v}) = \sum_{T \in \mathfrak{T}_h} \|\sqrt{\mu}\boldsymbol{\epsilon}(\mathbf{v}_h)\|_{0,T}^2 + \sum_{T \in \mathfrak{T}_h} \|\sqrt{\lambda}\,\mathrm{div}\,\mathbf{v}_h\|_{0,T}^2$$

$$- (1 - \epsilon)\sum_{e \in \mathcal{E}_h} \int_e \{\boldsymbol{\sigma}(\mathbf{v}_h) \cdot \mathbf{n}\}[\mathbf{v}_h]\,ds + \sum_{e \in \mathcal{E}_h}\Big(\frac{\tau_1}{h}\|\mathbf{v}_h\|_{0,e}^2 + \frac{\tau_2}{h}\|\mathbf{v}_h \cdot \mathbf{n}\|_{0,e}^2\Big)$$

$$\geq \Big(\underline{\mu} - \frac{\gamma_1}{2}(1-\epsilon)\Big)\sum_{T \in \mathfrak{T}_h} \|\boldsymbol{\epsilon}(\mathbf{v}_h)\|_{0,T}^2 + \Big(1 - \frac{\gamma_2}{2}(1-\epsilon)\Big)\sum_{T \in \mathfrak{T}_h} \|\sqrt{\lambda}\,\mathrm{div}\,\mathbf{v}_h\|_{0,T}^2$$

$$+ \Big(\tau_1 - \frac{\overline{\mu}C_N C_0}{2\gamma_1}(1-\epsilon)\Big)\sum_{e \in \mathcal{E}_h} \frac{1}{h}\int_e [\mathbf{v}_h]^2 + \Big(\tau_2 - \frac{C_N C_0}{2\gamma_2}(1-\epsilon)\Big)\sum_{e \in \mathcal{E}_h} \frac{1}{h}\int_e [\mathbf{v}_h \cdot \mathbf{n}]^2.$$

Take $\gamma_1 = \frac{\mu}{1-\epsilon}$ and $\gamma_2 = \frac{1}{1-\epsilon}$. Then the conclusion follows with

$$C_A = \min\Big\{\frac{\underline{\mu}}{2}, \frac{1}{2}, \tau_1 - \frac{\overline{\mu}C_N C_0}{2\underline{\mu}}(1-\epsilon)^2, \tau_2 - \frac{C_N C_0}{2}(1-\epsilon)^2\Big\}$$

for $\tau_1 > \frac{\overline{\mu}C_N C_0}{2\underline{\mu}}(1-\epsilon)^2$ and $\tau_2 > \frac{C_N C_0}{2}(1-\epsilon)^2$. $\qquad\square$

Remark 4.9. The choice of parameter τ_1 depends on μ. However, τ_2 is independent of either μ or λ. So, we can choose τ_1 and τ_2 independent of λ including the nearly incompressible case. Let us look closely at the choice of τ^1. As we pointed out in the proof of Lemma 4.8, τ_1 should be larger than $C(\overline{\mu}/\underline{\mu})$ for some C. However, choosing τ_1 the same constant on the whole domain Ω makes the condition number grow when the ratio $\overline{\mu}/\underline{\mu}$ is large. In practice, it is sufficient to choose the value of τ_1 on each edge e as

$$\tau_1|_e = \kappa_1\left(\frac{\mu|_e}{\underline{\mu}}\right) \quad \text{for some } \kappa_1 > 0.$$

Lemma 4.10. *There exists constant $C_C > 0$ such that $a_h(\mathbf{u}_h, \mathbf{v}_h) \leq C_C\|\mathbf{u}_h\|_{E_h}\|\mathbf{v}_h\|_{E_h}$ holds for all $\mathbf{u}_h, \mathbf{v}_h \in \widehat{\mathbf{U}}_h$.*

Proof. By the Cauchy–Schwarz inequality, we have

$$a_h(\mathbf{u}_h, \mathbf{v}_h) \leq \sqrt{a_h(\mathbf{u}_h, \mathbf{u}_h)}\sqrt{a_h(\mathbf{v}_h, \mathbf{v}_h)}.$$

Hence, it suffices to show that there is constant $C > 0$ such that $a_h(\mathbf{v}_h, \mathbf{v}_h) \leq C\|\mathbf{v}_h\|_{E_h}^2$ for all $\mathbf{v}_h \in \widehat{\mathbf{U}}_h$. For the case when $\epsilon = 1$, there is nothing to prove. Suppose $\epsilon = -1$ or $\epsilon = 0$. By the same techniques used in the proof of Lemma 4.8, we have

$$a_h(\mathbf{v}_h, \mathbf{v}_h) \leq \left(\overline{\mu} + \frac{\gamma_1}{2}(1-\epsilon)\right)\sum_{T\in\mathcal{T}_h}\|\boldsymbol{\epsilon}(\mathbf{v}_h)\|_{0,T}^2 + \left(1 + \frac{\gamma_2}{2}(1-\epsilon)\right)\sum_{T\in\mathcal{T}_h}\|\sqrt{\lambda}\operatorname{div}\mathbf{v}_h\|_{0,T}^2$$
$$+ \left(\tau_1 + \frac{\mu C_N C_0}{2\gamma_1}(1-\epsilon)\right)\sum_{e\in\mathcal{E}_h}\frac{1}{h}\int_e[\mathbf{v}_h]^2 + \left(\tau_2 + \frac{C_N C_0}{2\gamma_2}(1-\epsilon)\right)\sum_{e\in\mathcal{E}_h}\frac{1}{h}\int_e[\mathbf{v}_h\cdot\mathbf{n}]^2$$

for all $\gamma_1 > 0$ and $\gamma_2 > 0$. Hence, the conclusion follows. $\square$

Now we prove the energy norm error estimate.

Theorem 4.11. *Let $\mathbf{u}$ and $\mathbf{u}_h$ be the solutions of* (2.1) *and* (3.4)*, respectively. Then we have*

$$\|\mathbf{u} - \mathbf{u}_h\|_{E_h} \leq Ch(\|\mathbf{u}\|_{\widetilde{H}^2(\Omega)} + \|\sqrt{\lambda}\operatorname{div}\mathbf{u}\|_{\widetilde{H}^1(\Omega)}).$$

Proof. By the triangular inequality, we have

$$\|\mathbf{u} - \mathbf{u}_h\|_{E_h} \leq \|\mathbf{u}_h - I_h\mathbf{u}\|_{E_h} + \|\mathbf{u} - I_h\mathbf{u}\|_{E_h}. \tag{4.3}$$

From Lemma 4.8 and Ceá's lemma, it follows that

$$\|\mathbf{u}_h - I_h\mathbf{u}\|_{E_h} \leq \frac{C_c}{C_A}\|\mathbf{u} - I_h\mathbf{u}\|_{E_h}. \tag{4.4}$$

By Theorem 4.3, (4.3) and (4.4), we have

$$\|\mathbf{u} - \mathbf{u}_h\|_{E_h} \leq \left(1 + \frac{C_c}{C_A}\right)C_I h(\|\mathbf{u}\|_{\widetilde{H}^2(\Omega)} + \|\sqrt{\lambda}\operatorname{div}\mathbf{u}\|_{\widetilde{H}^1(\Omega)}). \qquad \square$$

We remark that the following H^2-stability [1, 30] holds for the elasticity problems if material constants μ and λ are continuous:

$$\|\mathbf{u}\|_{\widetilde{H}^2(\Omega)} + \frac{1}{1-2\nu}\|\operatorname{div}\mathbf{u}\|_{\widetilde{H}^1(\Omega)} \leq C\|\mathbf{f}\|_{L^2(\Omega)} \quad \text{for some } C > 0. \tag{4.5}$$

To the authors' best knowledge, it is not known whether this type of estimate holds for the heterogeneous material. So, if the H^2-stability of type (4.5) holds for heterogeneous material case also, then the following result holds.

Remark 4.12. Assume that the H^2-stability argument (4.5) holds. Then there is a constant $C > 0$ such that $\|\mathbf{u} - \mathbf{u}_h\|_{E_h} \leq Ch\|\mathbf{f}\|_{L^2(\Omega)}$ holds for all λ. In addition, we can obtain the L^2-error estimate

$$\|\mathbf{u} - \mathbf{u}_h\|_{L^2(\Omega)} \leq Ch^2\|\mathbf{f}\|_{L^2(\Omega)}$$

by the standard duality argument.

Case	μ^+	μ^-	v	λ^+	λ^-	r_0
1	1	100	0.3	1.5	150	0.65
2	1	10	0.49	49	490	0.4
3	1	10	0.499	499	4990	0.4
4	1	10	0.4999	4999	49990	0.4
5	1	100	0.499	499	49900	0.6
6	1	1000	0.499	499	499000	0.6

Table 1: The parameters μ, v, λ and r_0 in cases 1–6.

5 Numerical Results

In this section, we provide some numerical experiments supporting our error estimates in Section 4. The domain is $\Omega = [-1, 1]^2$. The numerical simulations are carried out on uniform triangulation $\mathcal{T}_h$ by right triangles having size $h = 2^{-k}$, $k = 3, 4, \ldots, 8$. We let the interface be the zero set of some function $L(x, y)$. Let $\Omega^- = \{(x, y) \in \Omega : L(x, y) < 0\}$ and $\Omega^+ = \{(x, y) \in \Omega : L(x, y) > 0\}$. We present three examples. In Example 5.1 and Example 5.2, the analytic solution is known. We present the results with various coefficients μ and λ including the nearly incompressible case. In Example 5.3, we simulate the driven cavity problem. For all tests, we use an IIPG type scheme ($\epsilon = 0$). Results of other schemes are similar. In all examples, we see that the proposed scheme is locking free.

Example 5.1. We choose the level set function $L(x, y) = x^2 + y^2 - r_0^2$ and the exact solution

$$\mathbf{u} = \left(\frac{1}{\mu}(x^2 + y^2 - r_0^2)y, -\frac{1}{\mu}(x^2 + y^2 - r_0^2)x \right).$$

We compute the numerical results for various values of μ, λ and r_0. We show the results for six cases with different coefficients.

The errors in L^2 and piecewise H^1-norms are given in Table 2–7 for case 1–6, respectively. We observe $\mathcal{O}(h^2)$ in L^2 and $\mathcal{O}(h)$ in H^1-norm for all cases.

Now we show how to choose the penalty parameters. As we mentioned in Remark 4.9, the threshold for parameter τ_1 to ensure coerciveness of $a_h(\cdot, \cdot)$ depends on μ, and the threshold for parameter τ_2 is independent of both μ and λ. Thus, we set the parameters as

$$\tau_1|_e = \kappa_1 \cdot \mu|_e, \quad \tau_2 = \kappa_2, \tag{5.1}$$

where $e \in \mathcal{E}_h$. We set $\kappa_1 = 2$ and $\kappa_2 = 2$ in all cases.

We see that the convergent rates in L^2 and H^1-norms are optimal for case 1 (Table 2). For cases 2, 3 and 4, the Poisson ratio approaches 0.5 ($v = 0.49, 0.499, 0.4999$). However, we see that the convergent rates in L^2 and H^1-norms are optimal (Tables 3, 4 and 5).

In case 5 and 6, the contrasts of μ^+ and μ^- are set to be different (1 vs 100, 1 vs 1000). We observe that the convergence rates are optimal again (Tables 6 and 7).

Thus, the numerical results show that our IFEM with the choice of penalty parameters (5.1) is robust for Poisson ratio and the scale of contrast of μ.

Comparison with CRIFEM

We compare the RCRIFEM with the CRIFEM in [18].

First, let us compare the dof. The dof of RCRIFEM is $4 \cdot (2^{k+1})^2 + 4 \cdot 2^{k+1} + 1$ and that of CRIFEM is $6 \cdot (2^{k+1})^2 + 4 \cdot 2^{k+1}$. For example, when $k = 8$, we see that the dof of RCRIFEM is about 66.71 % of that of CRIFEM.

We graph the L^2 and H^1-errors versus the dof for both the methods in Figure 4. Both the x-axis and y-axis are in $\log_2$ scale. We chose the problem parameters as $\mu^+ = 1$, $\mu^- = 100$, $v = 0.499$, $r_0 = 0.6$. We see that

$1/h$	$\|u - u_h\|_{L_2(\Omega)}$	order	$\|u - u_h\|_{1,h}$	order
8	1.231×10^{-2}		3.733×10^{-1}	
16	3.087×10^{-3}	1.995	1.870×10^{-1}	0.998
32	7.791×10^{-4}	1.986	9.352×10^{-2}	1.000
64	1.980×10^{-4}	1.976	4.679×10^{-2}	0.999
128	5.077×10^{-5}	1.963	2.341×10^{-2}	0.999
256	1.330×10^{-5}	1.933	1.172×10^{-2}	0.998

Table 2: (Example 5.1) $\mu^+ = 1$, $\mu^- = 100$, $\nu = 0.3$, $r_0 = 0.65$.

$1/h$	$\|u - u_h\|_{L_2(\Omega)}$	order	$\|u - u_h\|_{1,h}$	order
8	1.627×10^{-2}		4.030×10^{-1}	
16	4.070×10^{-3}	1.999	2.011×10^{-1}	1.003
32	1.019×10^{-3}	1.998	1.005×10^{-1}	1.001
64	2.550×10^{-4}	1.998	5.025×10^{-2}	1.000
128	6.382×10^{-5}	1.998	2.513×10^{-2}	0.999
256	1.609×10^{-5}	1.988	1.257×10^{-2}	1.000

Table 3: (Example 5.1) $\mu^+ = 1$, $\mu^- = 10$, $\nu = 0.49$, $r_0 = 0.4$.

$1/h$	$\|u - u_h\|_{L_2(\Omega)}$	order	$\|u - u_h\|_{1,h}$	order
8	1.691×10^{-2}		4.050×10^{-1}	
16	4.230×10^{-3}	1.999	2.019×10^{-1}	1.004
32	1.058×10^{-3}	1.999	1.008×10^{-1}	1.001
64	2.647×10^{-4}	1.999	5.042×10^{-2}	1.000
128	6.622×10^{-5}	1.999	2.521×10^{-2}	1.000
256	1.666×10^{-5}	1.991	1.261×10^{-2}	0.999

Table 4: (Example 5.1) Nearly incompressible case, $\mu^+ = 1$, $\mu^- = 10$, $\nu = 0.499$, $r_0 = 0.4$.

$1/h$	$\|u - u_h\|_{L_2(\Omega)}$	order	$\|u - u_h\|_{1,h}$	order
8	1.699×10^{-2}		4.052×10^{-1}	
16	4.249×10^{-3}	1.999	2.019×10^{-1}	1.005
32	1.062×10^{-3}	2.000	1.009×10^{-1}	1.001
64	2.658×10^{-4}	1.999	5.044×10^{-2}	1.000
128	6.650×10^{-5}	1.999	2.522×10^{-2}	1.000
256	1.674×10^{-5}	1.990	1.262×10^{-2}	0.999

Table 5: (Example 5.1) Nearly incompressible case, $\mu^+ = 1$, $\mu^- = 10$, $\nu = 0.4999$, $r_0 = 0.4$.

$1/h$	$\|u - u_h\|_{L_2(\Omega)}$	order	$\|u - u_h\|_{1,h}$	order
8	1.730×10^{-2}		3.960×10^{-1}	
16	4.236×10^{-3}	2.030	1.961×10^{-1}	1.014
32	1.053×10^{-3}	2.008	9.789×10^{-2}	1.003
64	2.619×10^{-4}	2.007	4.885×10^{-2}	1.003
128	6.554×10^{-5}	1.998	2.441×10^{-2}	1.001
256	1.646×10^{-5}	1.993	1.221×10^{-2}	1.000

Table 6: (Example 5.1) Nearly incompressible case, $\mu^+ = 1$, $\mu^- = 100$, $\nu = 0.499$, $r_0 = 0.6$.

$1/h$	$\|u - u_h\|_{L_2(\Omega)}$	order	$\|u - u_h\|_{1,h}$	order
8	3.320×10^{-2}		4.524×10^{-1}	
16	6.744×10^{-3}	2.300	2.058×10^{-1}	1.137
32	1.158×10^{-3}	2.542	9.918×10^{-2}	1.053
64	2.777×10^{-4}	2.060	4.918×10^{-2}	1.012
128	6.657×10^{-5}	2.061	2.447×10^{-2}	1.007
256	1.664×10^{-5}	2.000	1.222×10^{-2}	1.002

Table 7: (Example 5.1) Nearly incompressible case, $\mu^+ = 1$, $\mu^- = 1000$, $\nu = 0.499$, $r_0 = 0.6$.

H^1-errors are almost the same, and we see that L^2 of RCRIFEM are slightly higher than that of CRIFEM. However, we see that the CPU time to solve the discretized systems from RCRIFEM is smaller than that of CRIFEM (Table 8). We used Matlab R2017a as a solver on a PC with an Intel® Core™ i7-3770 CPU at 3.40 GHz processor. Thus, there is a reasonable trade-off between the accuracy and the computational complexity.

Example 5.2. We choose the level set function $L(x, y) = x^2 + y^2/2 - 0.3$ and the exact solution

$$\mathbf{u} = \left(\frac{1}{\mu}\left(x^2 + \frac{y^2}{2} - 0.3 \right)y + 2y, \ -\frac{1}{\mu}\left(x^2 + \frac{y^2}{2} - 0.3 \right)x - 2x \right).$$

We set $\mu^+ = 1$ and $\mu^- = 100$. We report the L^2 and piecewise H^1-errors for the case of $\nu = 0.4$ and $\nu = 0.4999$ in Table 9 and Table 10, respectively. We see that the convergence rates are optimal for both cases. We observe that the result for the nearly incompressible case ($\nu = 0.4999$) is non-locking.

Example 5.3 (Driven cavity). We choose the level set function $L(x, y) = x^2 + y^2 - 0.4^2$. We impose the boundary condition

$$\begin{cases} \mathbf{u} = (0, 0) & \text{on } x = -1 \text{ or } x = 1, \text{ or } y = -1, \\ \mathbf{u} = (1, 0) & \text{on } y = 1. \end{cases}$$

We set $\mu^+ = 100$ and $\mu^- = 1$. We present the velocity fields for the cases $\nu = 0.49$ and $\nu = 0.4999$ in Figure 5.

	CPU time (s)	
$1/h$	**RCRIFEM**	**CRIFEM**
8	1.104	2.130
16	1.853	2.431
32	4.147	5.972
64	13.103	18.055
128	51.639	74.103
256	229.516	331.227

Table 8: Comparison of CPU time to solve the discretized system for RCRIFEM and CRIFEM.
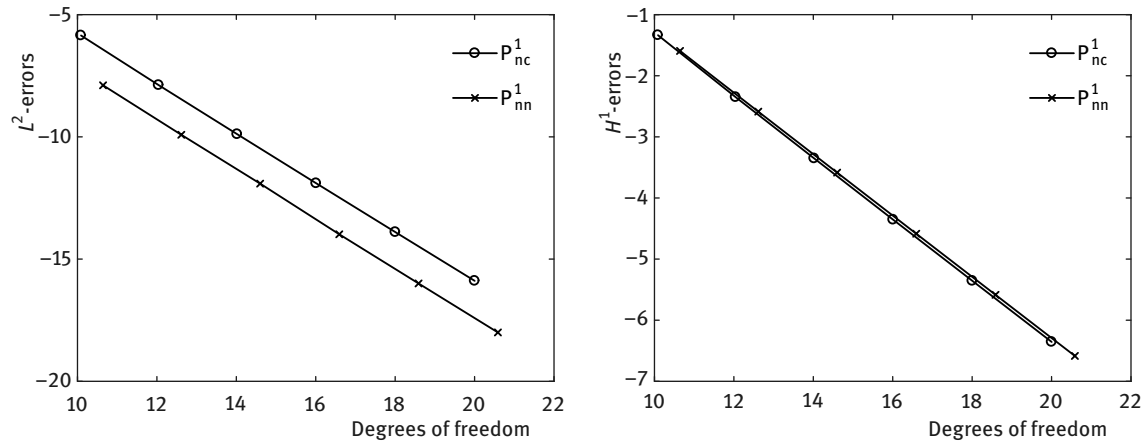
Figure 4: Comparison of L^2 and H^1-errors of RCRIFEM and CRIFEM in a $\log_2$ scale.

$1/h$	$\|u - u_h\|_{L_2(\Omega)}$	order	$\|u - u_h\|_{1,h}$	order
8	1.990×10^{-2}		5.325×10^{-1}	
16	5.175×10^{-3}	1.943	2.669×10^{-1}	0.997
32	1.304×10^{-3}	1.989	1.336×10^{-1}	0.998
64	3.293×10^{-4}	1.986	6.686×10^{-2}	0.999
128	8.362×10^{-5}	1.977	3.345×10^{-2}	0.999
256	2.145×10^{-5}	1.963	1.674×10^{-2}	0.999

Table 9: (Example 5.2) $\mu^+ = 1$, $\mu^- = 100$, $v = 0.4$.

$1/h$	$\|u - u_h\|_{L_2(\Omega)}$	order	$\|u - u_h\|_{1,h}$	order
8	2.514×10^{-2}		5.461×10^{-1}	
16	6.105×10^{-3}	1.943	2.711×10^{-1}	1.010
32	1.497×10^{-3}	1.989	1.352×10^{-1}	1.003
64	3.712×10^{-4}	1.986	6.763×10^{-2}	1.000
128	9.278×10^{-5}	1.977	3.382×10^{-2}	1.000
256	2.379×10^{-5}	1.963	1.691×10^{-2}	1.000

Table 10: (Example 5.2) $\mu^+ = 1$, $\mu^- = 100$, $v = 0.4999$.
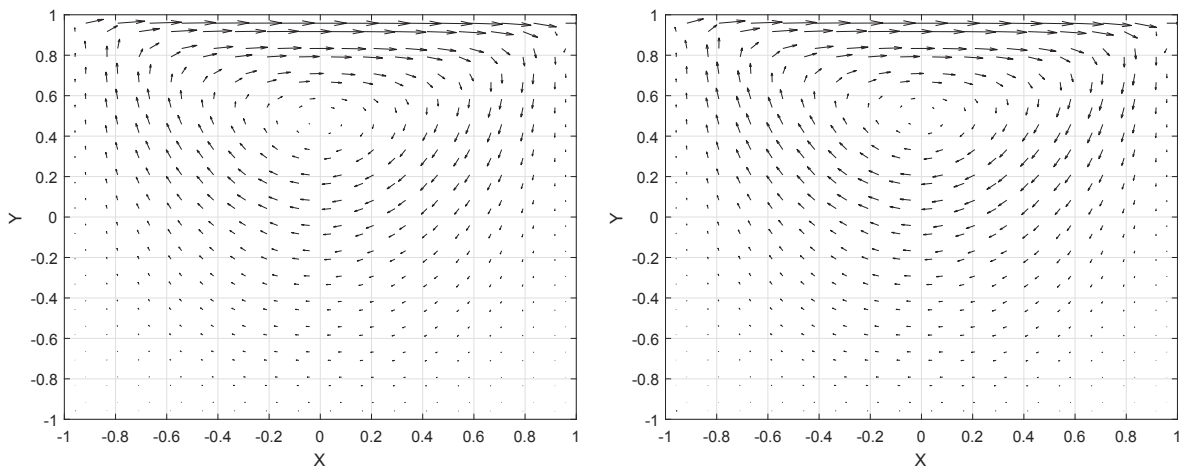
Figure 5: Numerical velocity field of driven cavity for the cases $v = 0.49$ (left) and $v = 0.4999$ (right).

6 Conclusion

We propose a new IFEM for the interface elasticity problems. We introduce RCRIFEM by modifying KS element to satisfy the balance of traction along the interface. We prove that our methods have optimal order of convergence in L^2 and piecewise H^1-norms. The dof of our schemes is about two thirds of a previous scheme [18], and we can choose penalty parameters independent of the Poisson ratio. In fact, one of the parameters depends on μ, and the other parameter is independent of both μ and λ.

The numerical results show that our methods are robust as the parameter λ goes to ∞.

A Appendix

We prove Proposition 3.1. Suppose a typical interface element T has vertices at $A(0, 0)$, $B(1, 0)$ and $C(0, 1)$. Assume that the interface meets with the edges at $D = (x_0, 0)$ and $E = (0, y_0)$ (Figure 6). Other cases can be treated similarly.
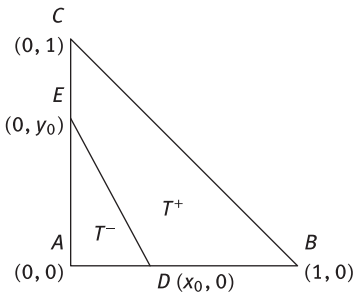
Figure 6: A typical reference interface triangle.

Let $\mathbf{c}_i = (a_i^+, b_i^+, c_i^+, a_i^-, b_i^-, c_i^-)$ ($i = 1, 2$) be the coefficients of $\widehat{\phi}$ in (3.1). Then conditions (3.2a), (3.2b) and (3.2c) give rise to

$$\begin{pmatrix} A & \mathbf{0} \\ \mathbf{0} & B \end{pmatrix}\begin{pmatrix} \mathbf{c}_1 \\ \mathbf{c}_2 \end{pmatrix} = \begin{pmatrix} \mathbf{g}_1 \\ \mathbf{g}_2 \end{pmatrix},$$

where 5×6 matrices A and B are respectively given by

$$\begin{pmatrix} 1 & \frac{1}{2} & \frac{1}{2} & 0 & 0 & 0 \\ 1 - y_0 & 0 & \frac{1}{2}(1 - y_0^2) & y_0 & 0 & \frac{1}{2}y_0^2 \\ 1 - x_0 & \frac{1}{2}(1 - x_0^2) & 0 & x_0 & \frac{1}{2}x_0^2 & 0 \\ -1 & -x_0 & 0 & 1 & x_0 & 0 \\ -1 & 0 & -y_0 & 1 & 0 & y_0 \end{pmatrix}, \quad \begin{pmatrix} 1 & 1 & 0 & 0 & 0 & 0 \\ 1 & 0 & 1 & 0 & 0 & 0 \\ 0 & 0 & 0 & 1 & 0 & 0 \\ 1 & x_0 & 0 & -1 & -x_0 & 0 \\ 1 & 0 & y_0 & -1 & 0 & -y_0 \end{pmatrix}. \quad \text{(A.1)}$$

Here, $\mathbf{g}_1 = [R_1, R_2, R_3, 0, 0]$ and $\mathbf{g}_2 = [V_1, V_2, V_3, 0, 0]^T$, where R_i is the edge average of the first component of $\widehat{\phi}$ and V_i is the nodal value of the second component. Furthermore, condition (3.2d) is written as

$$\begin{pmatrix} \mathbf{d}_1^T & \mathbf{d}_2^T \\ \mathbf{e}_1^T & \mathbf{e}_2^T \end{pmatrix}\begin{pmatrix} \mathbf{c}_1 \\ \mathbf{c}_2 \end{pmatrix} = \begin{pmatrix} 0 \\ 0 \end{pmatrix}, \quad \text{(A.2)}$$

where $\mathbf{n} = (n_1, n_2) = (y_0/\sqrt{x_0^2 + y_0^2}, x_0/\sqrt{x_0^2 + y_0^2})$ and

$$\mathbf{d}_1^T = (0, (2\mu^+ + \lambda^+)n_1, \mu^+ n_2, 0, -(2\mu^- + \lambda^-)n_1, -\mu^- n_2) := (d_{1i})_{i=1}^6,$$
$$\mathbf{d}_2^T = (0, \mu^+ n_2, \lambda^+ n_1, 0, -\mu^- n_2, -\lambda^- n_1) := (d_{2i})_{i=1}^6,$$
$$\mathbf{e}_1^T = (0, \lambda^+ n_2, \mu^+ n_1, 0, -\lambda^- n_2, -\mu^- n_1) := (e_{1i})_{i=1}^6,$$
$$\mathbf{e}_2^T = (0, \mu^+ n_1, (2\mu^+ + \lambda^+)n_2, 0, -\mu^- n_1, -(2\mu^- + \lambda^-)n_2) := (e_{2i})_{i=1}^6.$$

Arranging the equations (A.1) and (A.2), we get the 12-by-12 systems

$$
M := \begin{pmatrix} A & \mathbf{0} \\ \mathbf{d}_1^T & \mathbf{d}_2^T \\ \mathbf{0} & B \\ \mathbf{e}_1^T & \mathbf{e}_2^T \end{pmatrix} \begin{pmatrix} \mathbf{c}_1 \\ \mathbf{c}_2 \end{pmatrix} = \begin{pmatrix} \mathbf{g}_1 \\ 0 \\ \mathbf{g}_2 \\ 0 \end{pmatrix}.
$$

It suffices to show that the determinant of M is nonzero. By adding columns 6, 5 and 4 to 3, 2 and 1, respectively, and using the row eliminations, we see that the determinant of M is the same as the determinant of the matrix

$$
M' := \left(\begin{array}{cc|c} U & 0 & \mathbf{0} \\ 0 & \overline{d}_{66} & \mathbf{d}_2^T \\ \hline \mathbf{0} & 0 & B \\ 0 & \overline{e}_{16} & \mathbf{e}_2^T \end{array} \right), \quad \text{where} \quad U := \begin{pmatrix} 1 & \frac{1}{2} & \frac{1}{2} & 0 & 0 \\ 0 & -\frac{1}{2} & 0 & y_0 & 0 \\ 0 & 0 & -\frac{1}{2} & x_0 & \frac{1}{2}x_0^2 \\ 0 & 0 & 0 & 1 & x_0 \\ 0 & 0 & 0 & 0 & -x_0 \end{pmatrix}.
$$

Here, $\overline{d}_{66}$ and $\overline{e}_{66}$ satisfy

$$
x_0 \overline{d}_{66} = -n_1 y_0 \{(2\mu^+ + \lambda^+)x_0 y_0 + (2\mu^- + \lambda^-)(1 - x_0 y_0)\} - x_0 n_2 \{\mu^+ x_0 y_0 + \mu^-(1 - x_0 y_0)\},
$$
$$
x_0 \overline{e}_{16} = -n_2 y_0 \{\lambda^+ x_0 y_0 + \lambda^-(1 - x_0 y_0)\} - n_2 x_0 \{\mu^+ x_0 y_0 + \mu^-(1 - x_0 y_0)\}.
$$

By applying row operations to rows 7–12 of M', we have

$$
M'' := \left(\begin{array}{cc|c} U & 0 & \mathbf{0} \\ 0 & \overline{d}_{66} & \mathbf{d}_2^T \\ \hline \mathbf{0} & 0 & C \\ 0 & \overline{e}_{16} & \end{array} \right), \quad \text{where} \quad C := \begin{pmatrix} 1 & 1 & 0 & 0 & 0 & 0 \\ 0 & -1 & 1 & 0 & 0 & 0 \\ 0 & 0 & 0 & 1 & 0 & 0 \\ 0 & 0 & x_0 - 1 & 0 & -x_0 & 0 \\ 0 & 0 & y_0 - 1 & 0 & 0 & -y_0 \\ 0 & 0 & e_{22} + e_{23} & 0 & e_{25} & e_{26} \end{pmatrix}.
$$

Here, it is easy to see that

$$
\sqrt{x_0^2 + y_0^2}\, \det(C) = y_0^2(x_0 \mu^+ + (1 - x_0)\mu^-) + 2x_0^2(y_0 \mu^+ + (1 - y_0)\mu^-) + x_0^2(y_0 \lambda^+ + (1 - y_0)\lambda^-).
$$

Lemma A.1. *The determinant of M is given by*

$$
\det(M) = \det(U)\{\overline{d}_{66}\det(C) + \overline{e}_{16}\text{cofac}\},
$$

where

$$
\text{cofac} = \det \begin{pmatrix} 0 & \mu^+ n_2 & \lambda^+ n_1 & 0 & -\mu^- n_2 & -\lambda^- n_1 \\ 1 & 1 & 0 & 0 & 0 & 0 \\ 0 & -1 & 1 & 0 & 0 & 0 \\ 0 & 0 & 0 & 1 & 0 & 0 \\ 0 & 0 & x_0 - 1 & 0 & -x_0 & 0 \\ 0 & 0 & y_0 - 1 & 0 & 0 & -y_0 \end{pmatrix}
$$
$$
= -\det \begin{pmatrix} \mu^+ n_2 & \lambda^+ n_1 & -\mu^- n_2 & -\lambda^- n_1 \\ -1 & 1 & 0 & 0 \\ 0 & x_0 - 1 & -x_0 & 0 \\ 0 & y_0 - 1 & 0 & -y_0 \end{pmatrix}
$$
$$
= x_0 y_0 (\mu^+ n_2 + \lambda^+ n_1) + (1 - x_0)y_0 \mu^- n_2 + \lambda^- n_1(1 - y_0)x_0.
$$

Proof. This can be obtained by expanding the determinants with respect to column 7 of M''. ☐

Proposition A.2. *The determinant of M is always positive.*

Proof. This can be proven directly by Lemma A.1 and the fact that

$$
\det(U) < 0, \quad \det(C) > 0, \quad \overline{d}_{66} < 0, \quad \overline{e}_{16} < 0, \quad \text{cofac} > 0. \qquad ☐
$$

References

[1] C. Bacuta and J. H. Bramble, Regularity estimates for solutions of the equations of linear elasticity in convex plane polygonal domains, *Z. Angew. Math. Phys.* **54** (2003), no. 5, 874–878.

[2] R. Becker, E. Burman and P. Hansbo, A Nitsche extended finite element method for incompressible elasticity with discontinuous modulus of elasticity, *Comput. Methods Appl. Mech. Engrg.* **198** (2009), no. 41–44, 3352–3360.

[3] T. Belytschko and T. Black, Elastic crack growth in finite elements with minimal remeshing, *Int. J. Numer. Methods Eng.* **45** (1999), 601–620.

[4] T. Belytschko, C. Parimi, N. Moës, N. Sukumar and S. Usui, Structured extended finite element methods for solids defined by implicit surfaces, *Int. J. Numer. Methods Eng.* **56** (2003), 609–635.

[5] J. H. Bramble and J. T. King, A finite element method for interface problems in domains with smooth boundaries and interfaces, *Adv. Comput. Math.* **6** (1996), no. 2, 109–138.

[6] S. C. Brenner, Korn's inequalities for piecewise H^1 vector fields, *Math. Comp.* **73** (2004), no. 247, 1067–1087.

[7] F. Brezzi and M. Fortin, *Mixed and Hybrid Finite Element Methods*, Springer Ser. Comput. Math. 15, Springer, New York, 1991.

[8] K. S. Chang and D. Y. Kwak, Discontinuous bubble scheme for elliptic problems with jumps in the solution, *Comput. Methods Appl. Mech. Engrg.* **200** (2011), no. 5–8, 494–508.

[9] S.-H. Chou, D. Y. Kwak and K. T. Wee, Optimal convergence analysis of an immersed interface finite element method, *Adv. Comput. Math.* **33** (2010), no. 2, 149–168.

[10] P. G. Ciarlet, *Mathematical Elasticity. Vol. I*, Stud. Math. Appl. 20, North-Holland, Amsterdam, 1988.

[11] R. S. Falk, Nonconforming finite element methods for the equations of linear elasticity, *Math. Comp.* **57** (1991), no. 196, 529–550.

[12] P. Hansbo and M. G. Larson, Discontinuous Galerkin methods for incompressible and nearly incompressible elasticity by Nitsche's method, *Comput. Methods Appl. Mech. Engrg.* **191** (2002), no. 17–18, 1895–1908.

[13] P. Hansbo and M. G. Larson, Discontinuous Galerkin and the Crouzeix–Raviart element: Application to elasticity, *M2AN Math. Model. Numer. Anal.* **37** (2003), no. 1, 63–72.

[14] S. Jin, D. Y. Kwak and D. Kyeong, A consistent immersed finite element method for the interface elasticity problems, *Adv. Math. Phys.* **2016** (2016), Article ID 3292487.

[15] G. Jo and D. Y. Kwak, Geometric multigrid algorithms for elliptic interface problems using structured grids, *Numer. Algorithms* **81** (2019), no. 1, 211–235.

[16] R. Kouhia and R. Stenberg, A linear nonconforming finite element method for nearly incompressible elasticity and Stokes flow, *Comput. Methods Appl. Mech. Engrg.* **124** (1995), no. 3, 195–212.

[17] P. Krysl and T. Belytschko, An efficient linear-precision partition of unity basis for unstructured meshless methods, *Comm. Numer. Methods Engrg.* **16** (2000), no. 4, 239–255.

[18] D. Y. Kwak, S. Jin and D. Kyeong, A stabilized P_1-nonconforming immersed finite element method for the interface elasticity problems, *ESAIM Math. Model. Numer. Anal.* **51** (2017), no. 1, 187–207.

[19] D. Y. Kwak and J. Lee, A modified P_1-immersed finite elemnt method, *Int. J. Pure Appl. Math.* **104** (2015), 471–494.

[20] D. Y. Kwak, K. T. Wee and K. S. Chang, An analysis of a broken P_1-nonconforming finite element method for interface problems, *SIAM J. Numer. Anal.* **48** (2010), no. 6, 2117–2134.

[21] D. Kyeong and D. Y. Kwak, An immersed finite element method for the elasticity problems with displacement jump, *Adv. Appl. Math. Mech.* **9** (2017), no. 2, 407–428.

[22] G. Legrain, N. Moës and E. Verron, Stress analysis around crack tips in finite strain problems using the eXtended finite element method, *Internat. J. Numer. Methods Engrg.* **63** (2005), no. 2, 290–314.

[23] D. Leguillon and E. Sánchez-Palencia, *Computation of Singular Solutions in Elliptic Problems and Elasticity*, John Wiley & Sons, Chichester, 1987.

[24] Z. Li, T. Lin, Y. Lin and R. C. Rogers, An immersed finite element space and its approximation capability, *Numer. Methods Partial Differential Equations* **20** (2004), no. 3, 338–367.

[25] Z. Li, T. Lin and X. Wu, New Cartesian grid methods for interface problems using the finite element formulation, *Numer. Math.* **96** (2003), no. 1, 61–98.

[26] T. Lin, Y. Lin and X. Zhang, Partially penalized immersed finite element methods for elliptic interface problems, *SIAM J. Numer. Anal.* **53** (2015), no. 2, 1121–1144.

[27] N. Moës, J. Dolbow and T. Belytschko, A finite element method for crack growth without remeshing, *Internat. J. Numer. Methods Engrg.* **46** (1999), no. 1, 131–150.

[28] B. Rivière and M. F. Wheeler, Optimal error estimates for discontinuous Galerkin methods applied to linear elasticity problems, *Comput. Math. Appl* **46** (2000), 141–163.

[29] R. Stenberg, A family of mixed finite elements for the elasticity problem, *Numer. Math.* **53** (1988), no. 5, 513–538.

[30] M. Vogelius, An analysis of the *p*-version of the finite element method for nearly incompressible materials. Uniformly valid, optimal error estimates, *Numer. Math.* **41** (1983), no. 1, 39–53.